Journal of Scientific Research & Reports
2(1): 460-473, 2013; Article no. JSRR.2013.032

SCIENCEDOMAIN *international*
www.sciencedomain.org

Optimization in Breast Lesions Detection via Integrated Statistical Approach

Luminita Moraru[1*], Simona Moldovanu[2] and Mirela Punga Visan[1,3]

[1]Department of Chemistry, Physics and Environment, Dunarea de Jos University of Galati, 111 Domneasca, 800201, Galati, Romania.
[2]Dumitru Motoc High School, 15 Milcov St., 800509, Galati, Romania.
[3]Aurel Vlaicu High School, 25 1 Decembrie 1918 St., 800511, Galati, Romania.

Authors' contributions

This work was carried out in collaboration between all authors. All authors participated in preparation of manuscript. Authors SM, MPV participated in the design and the administration of the study and drafted the manuscript. Author LM participated in the interpretation and supervision of the results, and the preparation of the final version of the manuscript. All authors read and approved the final manuscript.

Research Article

Received 18th March 2013
Accepted 14th June 2013
Published 13th July 2013

ABSTRACT

Aims: The main purpose of this research was to develop a new method to extract the most valuable texture features to differentiate between cyst and solid nodule classes in breast echography images. *T*-test coupled with leave-one-out cross-validation analysis technique was developed. This technique was used to a breast ultrasound image database in order to select a small number of highly predictive features and to allow algorithms to operate effectively and faster.
Study Design: The image processing was made using the Matlab environment and statistical analysis was accomplished by using the SPSS ver. 17 software.
Place and Duration of Study: Department of Echography, St Maria's Hospital, Galati, between November and December 2011.
Methodology: To reach this goal, a feature extraction method was developed based on the geometric and statistical moments. Features extraction has been successfully accomplished and their further application has been based on an integrated statistical approach. To determine the meaningful features and their efficiency in each studied class, the statistical *T*-test was carried out. *T*-score was performed to establish the capability of

**Corresponding author: E-mail: luminita.moraru@ugal.ro;*

the features to differentiate between classes and also, as a ranking tool for features. In order to analyze if our results would lead to an independent data set, the leave-one-out cross-validation method has been used.
Results: Experimental results showed that the proposed method is very effective and the selected feature subsets could be used to compare the ability to differentiate between classes. Also the minimum size of the feature subsets was another pursued goal. Three different combinations of the statistical and geometric moment features could characterize the breast nodule (i.e. rectangularity, area convexity and the second order moment) and other three could characterize the breast cyst (i.e. circularity, form factor and eccentricity).
Conclusion: Through this method, the dimensionality of the feature vectors was substantial reduced and the ability to differentiate between cyst and solid nodule classes in breast echography images was improved.

Keywords: Statistical moment; geometric moment; t-test; t-score; leave-one-out cross-validation.

1. INTRODUCTION

Breast cancer remains the main cause of newly diagnosed cases of cancer and the second cause of cancer-related mortality of women in the United Stated and worldwide [1]. Moreover, in 2011 United State, about 1% of all breast cancers occurred among men [2]. Despite the screening and radiographic breast imaging performed, 10 to 30% of the malignant cases are not detected for various reasons.

Numerous selection and classification methods have been studied for accurate lesion boundary detection and an improved classification system for breast lesions. Keyvanfard et al. [3] reported a method based on feature selection of breast MRI lesions using a multi-classifier to increase accuracy and specificity of breast cancer detection. They reported a perfect classification of databases but, there is no information related to the computational cost and processing speed of the method. To detect the major differences between benign and malignant tumours, besides Chebyshev moments and log-polar transformation, Vyas and Rege used geometric moments [4]. Maitra et al. [5] used the gray level co-occurrence matrix (GLCM) features to abnormal masses identification in mammograms and Sheshadri et al. [6] classified the mammogram breast tissues by using the intensity histogram features. Kekre et al. [7] proposed a segmentation technique based on texture features. In [8] three different feature extraction methods (intensity histogram, GLCM and intensity based features) for classification of normal and abnormal patterns in mammogram were presented.
The aim of the present study was to develop an efficient method to extract the most valuable texture features to differentiate between cyst and solid nodule classes in breast echography images. We looked for the minimum number of the meaningful features able to characterize datasets and discriminate their components (i.e. accurately distinguish lesion/non-lesion or benign/malignant). The challenge is the choice of the best attributes or features of the recognition algorithms. The number of available variables leads to a very large number of possible choices. The secret of success in pattern recognition and classification is precisely to reduce this huge number of possibilities and to choose the most meaningful features "suggested" by the image. In order to reduce the computational costs, the proposed method integrates the information furnished by the statistical and geometric moments with the discriminately capability of *T*-test, *T*-score, and leave-one-out cross-validation methods. A novel sequential-elimination technique allows to identify and remove the irrelevant and redundant features was tested. We report five statistical moments and one geometrical

moment as meaningful features for image classification. These results lead in a decrease in feature dimensionality and in an increase in performance of classification and allow algorithms to operate faster and more effectively.

2. MATERIALS AND METHODS

To implement the proposed system, the following four steps were performed: i) de-noising operation; ii) segmentation of Regions of Interest ROIs (cysts and solid nodules) from surrounding background using active contour method; iii) analysis of the ROIs using statistical and geometric moments; iv) interpretation of the salient moments using statistical method.

2.1 Materials

The study comprised 52 patients. 28 patients were diagnosed with breast cysts and 24 with solid breast nodules. A cyst is a closed sac that contains fluids, gas or semi solid substances and a solid nodule is a mass of tissue that has to be made visible by ultrasounds. Almost 90% of all cysts on the human body are benign but the chances of a nodule being cancerous are higher. In this study, because our suspicious biological objects are not confirmed by biopsy as being tumours, we refer to them as “solid nodules”.

Fig. 1 presents certain examples of the acquired images. They were acquired using an SLE 401 echography medical device and a linear probe with a frequency of 6.5–9 MHz. They are bitmap images whose dimensions are 524×512 pixels and 8 bit/pixel. The images were processing by using the Matlab software ver. 2009a and an Intel Core I3 CPU, 4-GB RAM as hardware platform. The statistical analysis was accomplished using the SPSS ver. 17 software.

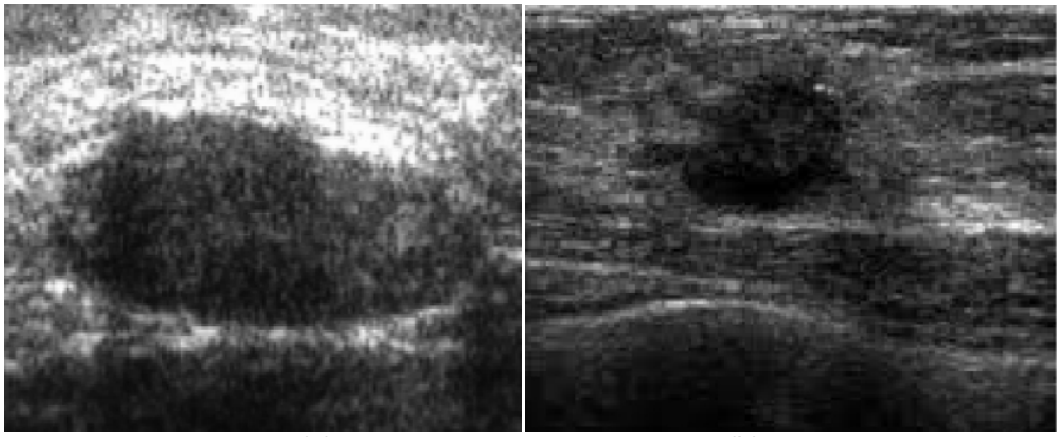

(a) (b)

Fig. 1. Typical breast ultrasound images; a) cyst; b) solid nodule

2.2 De-Noising Images

The Wiener filter is commonly used to restore linearly degraded images, and it is based on the minimum squared error. The frequency response of the non-causal Wiener filter is:

$$H(w) = \frac{P_s(w)}{P_s(w) + P_N(w)} \tag{1}$$

where $P_s(w)$ and $P_N(w)$ represent the power spectral density of the true signal and noise, respectively [9]. Results obtained by Wiener filtering achieve the best signal to noise ratios than other filtering methods.

2.3 Segmentation

The active contour methods (ACMs) for image segmentation allow a contour to accommodate to variability of the biological structures [10-12]. The ACM approach has been successfully applied to automatically detect benign and malignant breast tumours [13]. In a 2D image analysis context, an active contour is a flat curve $S(u) = I[x(u), y(u)]$, $u \in [0, 1]$, which can dynamically change its shape and fit itself to image elements such as edges or borders. The total energy of the ACM [14]:

$$E = \int_0^1 [E_{\text{int}}(S(u)) + E_{img}(S(u)) + E_{con}(S(u))]du, \tag{2}$$

comprises the internal energy of the spline $E_{\text{int}}(S(u))$, the image energy $E_{img}(S(u))$ and, the external constraint forces $E_{con}(S(u))$. $E_{\text{int}}(S(u))$ is composed of the first and second order derivatives controlled by weighing parameters α (the elasticity parameter of the snake) and β (the rigidity parameter of the snake):

$$E_{\text{int}} = \frac{\alpha}{2} \underbrace{\left| \frac{\partial}{\partial u} S(u) \right|^2}_{Elastic\ \ energy} + \frac{\beta}{2} \underbrace{\left| \frac{\partial^2}{\partial u^2} S(u) \right|^2}_{Bending\ energy} \tag{3}$$

Image energy E_{img} is used to drive the contour towards the desired boundaries.

2.4 Statistical Moments

In an image, moments of all orders exist and a complete moment set able to describe the information contained in the image can be computed. However, the access to all the relevant information contained in an image would require handling with an infinite number of moment values. So, the challenge is to select only a meaningful subset of the moment values that contains sufficient information for a unique and complete characterization of an image. Usually, the statistical moments are used as texture classification methods [15-18]. Let *z* be a random variable denoting the gray value and $p(z_i), i = 0, 1, 2, ..., L-1,$ the corresponding histogram, where *L* is the number of the distinct gray levels. Table 1 presents the statistical moments used in our analysis.

Table 1. Statistical moments [19]

The *n*th moment of *z* about mean	$\mu_n = \sum_{i=0}^{L-1} (z_i - m)^n p(z_i)$	$m = \sum_{i=0}^{L-1} z_i p(z_i) = \mu_1$ is the first order moment or mean value of *z*.
The second moment (or variance)	$\sigma^2(z) = \mu_2(z)$	It furnishes the description of relative smoothing of distribution.
The third moment (or skewness)	$\mu_3(z) = \sum_{i=0}^{L-1} (z_i - m)^3 p(z_i)$	It is a measure of the lopsidedness of the distribution.
The fourth moment	$\mu_4(z) = \sum_{i=0}^{L-1} (z_i - m)^4 p(z_i)$	It is a measure of its relative flatness.

These moments have been computed using Matlab functions and evaluated for various breast echography images.

2.5 Geometric Moments

The geometric moments are widely used as shape features of biological objects in echographic images. They present a low computational cost but are highly sensitive to noise [20]. For a *N* x *N* digital image *I*(*x*, *y*), the 2D moments are:

$$M_{pq} = \sum_x \sum_y \left[x^p x^q I(x,y) \right] \tag{4}$$

where $p,q = 1, 2, ..., \infty$. Based on the *p* and *q* values, Table 2 presents both the moments and the derived features used in the present study. These features represent a better way to investigate the abnormalities in breast tissue having arbitrary shapes [21].

Table 2. Geometric moments and the derived features [20]

Moments		Features	
$m_{00} = \sum_x \sum_y \left[x^0 y^0 I(x,y)\right] = \sum_x \sum_y \left[I(x,y)\right]$	It is the total area of a binary image	$OR = \frac{1}{2}\tan^{-1}\left(\frac{2m_{11}}{m_{20} - m_{02}}\right)$	Orientation
$m_{10} = \sum_x \sum_y \left[x^1 y^0 I(x,y)\right] = \sum_x \sum_y \left[xI(x,y)\right]$ $m_{01} = \sum_x \sum_y \left[x^0 y^1 I(x,y)\right] = \sum_x \sum_y \left[yI(x,y)\right]$	They are centre of the image *I(x,y)*. The coordinates of the centre of mass are: $\bar{x} = m_{10}/m_{00}$ $\bar{y} = m_{01}/m_{00}$.	$AR = \frac{length_{bounding\_box}}{width_{bounding\_box}} = \frac{LB}{WB}$	Aspect ratio $length_{bounding\_box} = LB$ and $width_{bounding\_box} = WB$ are the dimensions of a smallest box containing the ROI
		$RT = \frac{m_{00}}{LB \times WB}$	Rectangularity
$m_{11} = \sum_x \sum_y \left[x^1 y^1 I(x,y)\right] = \sum_x \sum_y \left[xyI(x,y)\right]$	They are the moments of inertia	$AC = \frac{m_{00}}{Area_{convex\_hull}}$	Area convexity (convex hull is the smallest convex region containing pixels)
$m_{20} = \sum_x \sum_y \left[x^2 y^0 I(x,y)\right] = \sum_x \sum_y \left[x^2 I(x,y)\right]$		$PC = \frac{Perimeter_{ROI}}{Perimeter_{convex\_hull}}$	Perimeter convexity
$m_{02} = \sum_x \sum_y \left[x^0 y^2 I(x,y)\right] = \sum_x \sum_y \left[y^2 I(x,y)\right]$		$CC = \frac{4\pi \times m_{00}}{Perimetr_{convex\_hull}}$	Circularity or the degree of roundness of ROI
		$EC = \frac{Axis\_Lenght_{long}}{Axis\_Lenght_{short}}$	Eccentricity or the ratio of the distance between the foci of the ellipse and its major axis length
		$FF = \frac{4\pi \times m_{00}}{Perimeter_{ROI}^{\ 2}}$	Form factor measures the ROI's compactness

3. RESULTS AND DISCUSSION

The segmentation of images was accomplished on the suspected lesion. Fig. 2 shows the segmentation results. To accurately detect the ROIs, the optimal $\alpha = 0.4$ and $\beta = 0.2$ values were used, and the number of iteration of the algorithm was n = 50.

The statistical moments were computed for each cropped sample as Fig. 3 shown. Their statistical values are stored in Table 3. According to *P*-value criterion, all proposed statistical moments are statistical significant.

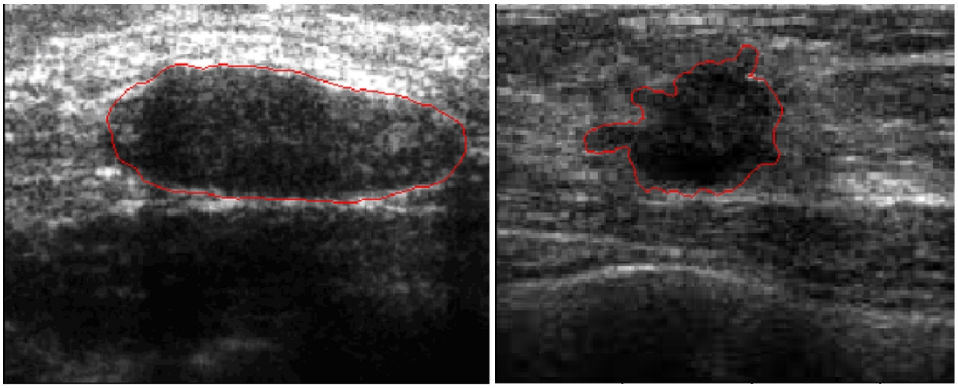

(a) (b)

Fig. 2. Contours detected by ACM; a) cyst; b) solid nodule

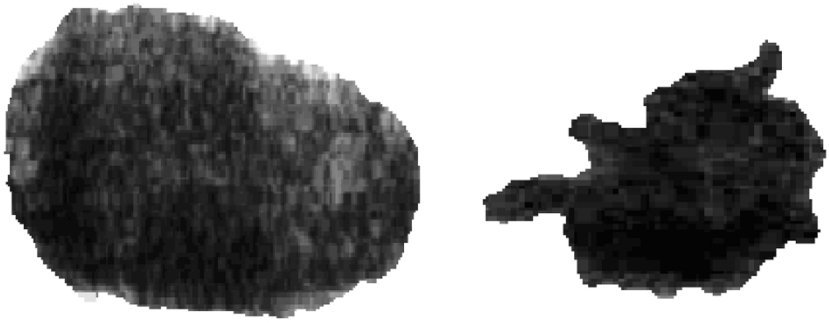

(a) (b)

Fig. 3. Cropped ROIs using the statistical moments' analysis; a) cyst; b) solid nodule

After the boundaries were detected and cropped, the next logical step is to transform the samples in binary images (Fig. 4). Further, the statistical features of the geometric moments were computed.

T - test was performed as a direct way to reduce the dimensionality of the dataset. It allowed estimating statistical significance of features and it performed a filtering of non-informative features. Also, we note that besides *P* - value, the statistical values as mean, standard deviation and standard error mean were also computed (Table 4).

Table 3. *T* - test results corresponding to the statistical moments of the detected ROIs

	Studied classes	95% confidence interval of the difference			
		Mean	Standard deviation	Standard error mean	*P*- value
μ_1	Nodules	192.07	27.22	7.97	0.004
	Cysts	177.42	42.68	13.03	
μ_2	Nodules	97.77	16.78	4.65	<0.002
	Cysts	112.54	15.22	5.1	
μ_3	Nodules	250.94	28.53	7.99	<0.001
	Cysts	232.58	43.68	13.32	
μ_4	Nodules	15.51	0.89	0.26	<0.002
	Cysts	14.64	1.92	0.7	

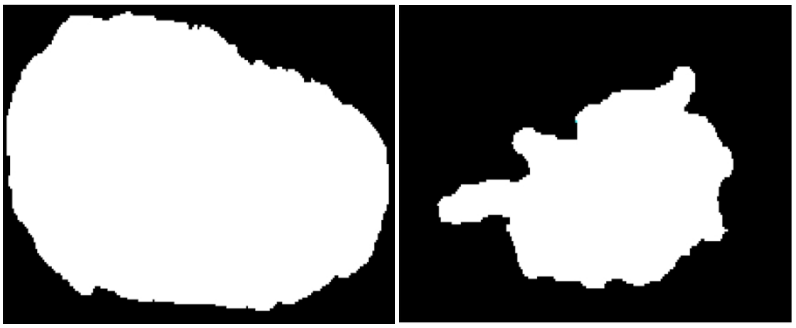

(a) (b)

Fig. 4. Binarized ROIs for geometrical moment analysis; a) cyst; b) solid nodule

Table 4. *T*-test results corresponding to the geometric moments of the detected ROIs

	Studied classes	95% confidence interval of the difference			
		Mean	Standard deviation	Standard error mean	*P* -value
m_{00}	Solid nodule	1.11e4	6.87e3	1.99e3	0.003
	Cyst	1.98e4	1.77e4	5.10e3	
OR	Solid nodule	14.37	33.25	9.58	**0.163**
	Cyst	2.78	8.96	2.59	
AR	Solid nodule	1.54	0.56	0.09	**0.988**
	Cyst	0.03	5.08	1.48	
RT	Solid nodule	1.55	0.71	0.20	<0.002
	Cyst	90.41	37.66	11.58	
AC	Solid nodule	1,09e4	6,48e3	1,88e3	0.002
	Cyst	1.7e4	1.47e4	3.76e3	
PC	Solid nodule	13.51	7.42	2.18	**0.141**
	Cyst	23.71	51.6	14.9	
CC	Solid nodule	0.45	0.18	0.05	<0.001
	Cyst	0.56	0.23	0.09	
EC	Solid nodule	0.73	0.12	0.06	<0.002
	Cyst	0.85	0.09	0.03	
FF	Solid nodule	0.6	0.15	0.05	<0.001
	Cyst	0.45	0.18	0.05	

Table 4 shows insignificant differences between the AR, OR and PC features and they are excluded as being non-significant and non-informative. The rest of the features were indicated as being appropriate for classification.

In order to evaluate the potentiality of textural analysis for classification purpose, a sequential feature selection method was developed by using *T* - score. The method encompasses the following steps:

i. A features vector $M = \{\mu_1, \mu_2, \mu_3, \mu_4, m_{00}, OR, AR, RT, AC, PC, CC, EC, FF\}$ has been set. It consists of 13 features.
ii. Only the features that meet the criteria imposed by *T* - test have been selected. A reduced set of features $M' = \{\mu_1, \mu_2, \mu_3, \mu_4, m_{00}, RT, AC, CC, EC, FF\}$ has been generated. This subset is sorted starting from the lowest value according to the *P* - values.
iii. In order to determine the weight of each feature for further classification task, the *T* - score has been used. Therefore, the features belong to the set M' were divided in two random subsets; one is labelled as 'test subset' and the second is the 'training subset'.
iv. The leave-one-out method has been used to verify the accuracy of the features selection procedure.

3.1 Features selection

T-score was used to measure the capability of each individual moment (statistical and geometric) and of each feature in differentiating between cyst and nodule samples and *vice versa*. t^C_{score} differentiates between cyst and nodule samples and t^N_{score} differentiates between nodule and cyst samples. The larger absolute t_{score} indicates strong discriminatory capability between studied classes. t^N_{score} and t^C_{score} are computed using the following two equations:

$$t^N_{score} = \frac{M_N - M^*_C}{\sqrt{\frac{(N_N - 1)\sigma^2_N + (N_{C^*} - 1)\sigma^2_{C^*}}{N_N + N_{C^*} - 2}\left(\frac{1}{N_N} + \frac{1}{N_{C^*}}\right)}} \quad (5)$$

where M_N and σ^2_N are the mean and variance, respectively of a particular feature, for test nodule samples; M_C and $\sigma^2_{C^*}$ are the mean and variance of the same feature, for cyst samples used for training. N_N and N_{C^*} represent the numbers of nodule test samples and cyst training samples, respectively.

$$t^C_{score} = \frac{M_C - M^*_N}{\sqrt{\frac{(N_C - 1)\sigma^2_N + (N_{N^*} - 1)\sigma^2_{C^*}}{N_C + N_{N^*} - 2}\left(\frac{1}{N_C} + \frac{1}{N_{N^*}}\right)}} \quad (6)$$

In a similar way, M_C and σ_C^2 are the mean and variance of a particular feature for all test cyst samples, M_N and $\sigma_{N^*}^2$ are the mean and variance of the same feature for training nodule samples, and N_C and N_{N^*} are the numbers of cyst test samples and nodule training samples, respectively. The computed values are stored in Table 5.

Table 5. Percentage value of t_{score}^N and t_{score}^C computed for nodule and cyst classes

	μ_1	μ_2	μ_3	μ_4	m_{00}	RT	AC	CC	EC	FF
t_{score}^N	**41.6**	61.3	**37.19**	**37.14**	57.6	86.3	75.1	57.8	59.21	**42.5**
t_{score}^C	**46.39**	**46.9**	**46.5**	**43.55**	54.9	53.3	58.35	91.18	61.43	64.9

The feature selection was carried out for set M'. In order to remove all redundant or irrelevant features and to avoid the overestimation of the classification results, an optimal threshold of 50% was imposed. T-score values less than 50% entail an abnormal distribution in the studied samples and those features have been removed from our analysis. The combinations $R_N = \{\mu_2, m_{00}, RT, AC, CC, EC\}$ for the solid nodule class and $R_C = \{m_{00}, RT, AC, CC, EC, FF\}$ for the cyst class respectively, provided the best discriminative accuracy.

3.2 Validation

The discriminative power of the selected features was tested by using the leave-one-out cross-validation method. Once again, the each dataset was randomly divided into two subsets. The rate of decay of the *T*-scores values in each studied class was assessed. Additionally, the variability of the scores and the stability of the feature ranking were studied.

The classification rates as a function of the number of observations (or features) *n* are plotted in Fig. 5. *n* is successively varied from 1 to 10. A larger value of *n* means a smaller training set and vice versa. When the size of the training set is large, the ranked features result in high rates. The leave-one-out cross-validation method validated the reliability of the feature vectors $R'_C = \{CC, FF, EC\}$ for breast cyst samples and $R'_N = \{RT, AC, \mu_2\}$ for breast nodule samples, respectively. Also, *T*-score higher than 60% characterizes those features which present the predictive ability to discriminate cyst by solid nodule. This is a very important result because different features are validated as meaningful for each studied class and any uncertainty is avoided.

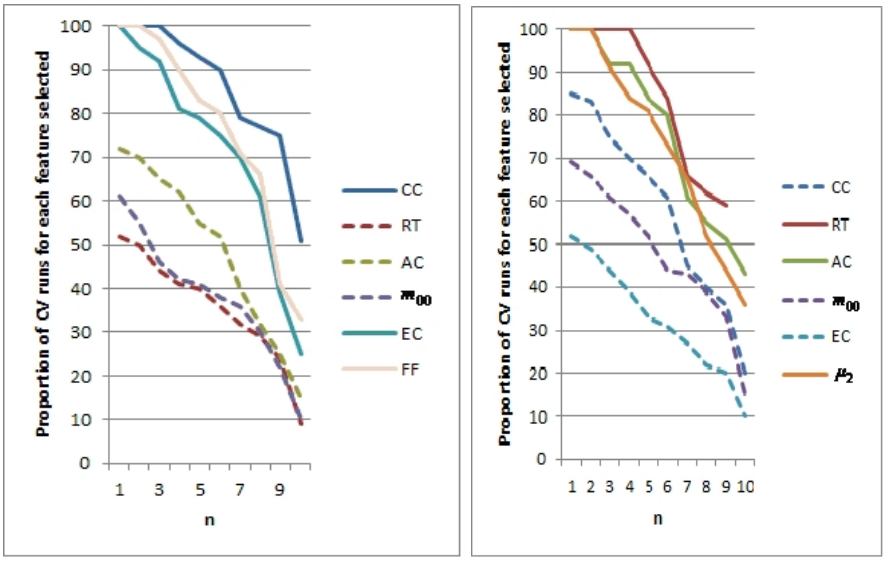

(a) (b)

Fig. 5. The accuracy of the features selection procedure with respect to the number of samples left out in leave-one-out experiments; the number of observations *n* is ranging from 1 to 10. The solid lines denote valid and meaningful features. The dashed lines correspond to the invalid features according to T-score results. (a) cyst samples, (b) solid nodule samples

Generally, in the feature classification operation, the correlation between samples may be lost due to inadequately sample size. Ideally, all features should be employed in the classifier design. However, some of them are not reliable for classification purposes and only a part of the initial set of features may be used. Assuming an adequate threshold of 50%, we conducted a ranking and validation analysis for our classes and we found that the breast cysts and solid nodules are related to five geometric moments and only one statistical moment.

As data stored in Table 5 show, for breast cyst lesions, the most salient feature is circularity CC ($t_{score} = 91.18$). It denotes anatomical circularity of the breast cyst. Usually, cyst masses are round in shape while nodule masses are more likely to be irregular or oval in shape. In the case of the breast solid nodule category, the rectangularity RT ($t_{score} = 86.3$) is the salient feature. A large RT denotes a bigger mass of the nodule compared with the area of the smallest box that surrounds the biological object.

Apparently, choosing the best feature set in order to maximize the performance of the classification is a time-consuming procedure but it is less time consuming than the method proposed by Keyvanfard et al. [3]. We tried to balance the time-consuming issue with the ability for classification and even to classification performance constrains. Furthermore, we investigated how the performance of the differentiation of the chosen features and training sample size are correlated. We avoided the unbalanced data sets (namely, 4 malignant and 26 benign lesions) reported in study [3] and we analyzed 28 breast cyst and 24 breast solid nodule samples. The large performance variations in the differentiation are mainly the result of the size of the data sets.

4. CONCLUSION

In many applications of pattern classification and computer vision, in order to classify the features in an image different kinds of moments are used. Through this study is further strengthened the idea that it is not always straightforward to determine *a priori* the optimal set of features suitable to characterize the breast cysts or nodules. The proposed method allows the selection of the valuable features and designs a low dimensional feature vectors able to differentiate between breast lesions. This system may be used as a second opinion tool by the radiologists.

Our future work will include the design and development of an expert system based on moment of image for breast lesions analysis. Furthermore, we will also try to form novel feature combinations, in which the selected features need not be the most highly ranked but rather more accurate. The system will furnish reliable information to differentiate between textural features of the breast lesions.

CONSENT

All authors declare that written informed consent was obtained from the patient for publication of this case report and accompanying images.

ETHICAL APPROVAL

All authors hereby declare that all experiments have been examined and approved by the appropriate ethics committee (Ref No 4775/28.02.2013) and have therefore been performed in accordance with the ethical standards laid down in the 1964 Declaration of Helsinki.

ACKNOWLEDGEMENTS

The author Simona Moldovanu would like to thank the Project SOP HRD-EFICIENT 61445/2009 of Dunarea de Jos University of Galati, Romania.

COMPETING INTERESTS

Authors have declared that no competing interests exist.

REFERENCES

1. Jemal A, Siegel R, Ward E, Murray T, Xu J, Thun MJ. Cancer statistics. CA Cancer J Clin. 2007;57(1):43-66.
2. American Cancer Society. Accessed 23 March 2012. Available: http://www.cancer.org/Research/CancerFactsFigures/index.
3. Keyvanfard F, Shoorehdeli MA, Teshnehlab M. Feature selection and classification of breast MRI lesions based on multi classifier, In: Proceedings of International Symposium on Artificial Intelligence and Signal Processing. Tehran, Iran. 2011;54-58.
4. Vyas VS, Rege PP. Malignancy texture classification in digital mammograms based on chebyshev moments and Logpolar transformation. International Journal on Bioinformatics and Medical Engineering. 2007;7(1):29-35.

5. Maitra IK, Nag S, Bandyopadhyay SK. Identification of abnormal masses in digital mammography images. International Journal of Computer Graphics. 2011;2(1):17-30.
6. Sheshadri HS, Kandaswamy A, Experimental investigation on breast tissue classification based on statistical feature extraction of mammograms. Comput. Med. Imaging Graph. 2007;31(1):46-48.
7. Kekre HB, Gharge S, Texture based segmentation using statistical properties for mammographic images. nternational Journal of Advanced Computer Science and Applications. 2010;1(5):102-107.
8. Nithya R, Santhi B. Comparative study on feature extraction method for breast cancer classification. Journal of Theoretical and Applied Information Technology. 2011;33(2):220-226.
9. Moldovanu S, Moraru L, Zerrad E, Biswar A. Speckle noise reduction methods in cardiac cycles. Int. J. Phys. Sci. 2012;7:797-804.
10. Su Y, Wang Jiao YJ, Guo Y. Automatic detection and classification of breast tumors in ultrasonic images using texture and morphological features. Open Med. Inform. J. 2011;5:26-37.
11. Liu B, Cheng HD, Huang JH, Tian JW, Liu JF, Tang XL. Automated segmentation of ultrasonic breast lesions using statistical texture classification and active contour based on probability distance. Ultrasound Med. Biol. 2009;35:1309-1324.
12. Hamarneh G, Gustavsson T. Combining snakes and active shape models for segmenting the human left ventricle in echocardiographic images. Proceeding of IEEE: Computers in Cardiology. Cambridge, MA-USA. 2000;27:115-118.
13. Huang YL, Chen DR. Automatic contouring for breast tumors in 2-D sonography. Ultrasound Med. Biol. 2004;30:625-632.
14. Kass M, Witkin A, Terzopoulos D, Snakes: Active contour models. Int. J. Comput. Vis. 1988;1:321-331.
15. Ahmadian A, Mostafa A, Abolhassani MD, Salimpour Y. A texture classification method for diffused liver diseases using Gabor wavelets. Proceedings of 27th Annual International Conference Engineering in Medicine and Biology Society IEEE-EMBS Berlin, Germany. 2005;2:1567-1570.
16. Raja KB, Madheswaran M, Thyagarajah K. Evaluation of tissue characteristics of kidney for diagnosis and classification using first order statistics and RTS invariants signal processing. Proceedings of International Conference Communications and Networking, Anna University, Chennai. 2007;483-487.
17. Sohail ASM, Rahman MM, Bhattacharya P, Krishnamurthy S, Mudur SP. Retrieval and classification of ultrasound images of ovarian cysts combining texture features and histogram moments. Proceedings of IEEE International Symposium on Biomedical Imaging, Rotterdam. 2010;288-291.
18. Kanakatte A, Mani N, Srinivasan B, Gubbi J. Pulmonary tumor volume detection from positron emission tomography images. Proceedings of International Conference Biomedical Engineering and Informatics, Sanya. 2008;2:213-217.
19. Nixon M. Aguano A. Feature extraction and Image Processing for Computer Vision. 3rd Ed. London: Elsevier Ltd; 2012.
20. Ghorbel F, Derrode S, Dhahbi S, Mezhoud R., Reconstructing with Geometric Moments. Proceedings of International Conference on Machine Intelligence, Tunisia; 2005.

21. Chaki J, Parekh R. Plant leaf recognition using shape based features and neural network classifiers, International Journal of Advanced Computer Science and Applications. 2011;2:41-47.

Peer-review history:
The peer review history for this paper can be accessed here:
http://www.sciencedomain.org/review-history.php?iid=176&id=22&aid=1654